

Unified Power Quality Conditioner (UPQC) with Voltage Dips and Over-voltages Compensation Capability

Víctor M. Moreno¹, Alberto Pigazo¹, Marco Liserre² and Antonio Dell'Aquila²

¹ Departamento de Electronica y Computadores
Universidad de Cantabria

Avda. de los Castros s/n, 39004 Santander (Spain)
Tel.:+34 942 201576, fax:+34 942 201303, e-mail: morenov@unican.es, pigazoa@unican.es

² Dipartimento di Elettrotecnica ed Elettronica
Politecnico di Bari

Via Orabona 4, 70125 Bari (Italy)
Tel.:+39 080 5963433 , fax:+39 080 5963410, e-mail: liserre@ieec.org, dellaqui@poliba.it

Abstract

Unified power quality conditioners (UPQCs) allow the mitigation of voltage and current disturbances that could affect sensitive electrical loads while compensating the load reactive power. Diverse control techniques have been proposed to evaluate the instantaneous output voltage of the series active power filter of the UPQC but, in most cases, these controllers only can compensate a kind of voltage disturbance.

This paper proposes a new digital controller for UPQCs which allows the load current harmonics and reactive power to be compensated at the grid side while avoiding the effect of voltage dips, over-voltages and voltage harmonics on the local loads. The controller characteristics can be established on-line without changing its basic structure. The performance of the proposed controller has been evaluated through simulation tests.

Keywords: UPQC, voltage dips, over-voltages, voltage harmonics, current harmonics, reactive component.

1. Introduction

Unified power quality conditioners (UPQCs) consist of combined series and shunt active power filters (APFs) for simultaneous compensation of voltage and current disturbances and reactive power. They are applicable to power distribution systems, being connected at the point of common coupling (PCC) of loads that generate harmonic currents. Diverse topologies has been proposed in literature for UPQCs in single-phase configurations, i.e. two IGBT half bridges [1] or multilevel topologies [2], but this paper focus on the commonly employed general structure depicted in figure 1 [3]. As can be seen, the power converters share a dc-bus and, depending on their functionalities, employ an isolation transformer (series APF) or an inductance (shunt APF) as voltage or current links.

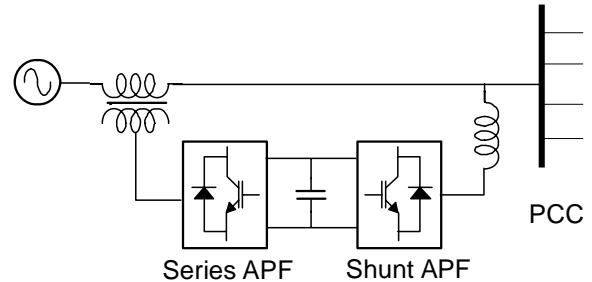


Fig. 1. Hardware structure of a UPQC.

The series APF must compensate the source voltage disturbances, such as harmonics, dips or over-voltages, which might deteriorate the operation of the local load while the shunt APF attenuates the undesirable load current components (harmonic currents and the fundamental frequency component which contributes to the reactive load power). Moreover, the shunt APF must control the dc-bus voltage in order to ensure the compensation capability of the UPQC [4].

These functionalities can be carried out by applying diverse control strategies which can operate in the time domain, in the frequency domain or both [5]. Time domain methods, such as pq or dq based methods [6]-[8], allow the fast compensation of time-variant disturbances but make more complex their selective compensation. In this sense, frequency domain methods are more flexible but their dynamical response is slower.

This paper proposes a new control technique for UPQCs based on a Kalman filtering approach. The proposed method operates both in the time and frequency domains allowing the selective compensation of voltage and current harmonics with fast dynamical responses. Moreover, the impact of dips and over-voltages can be attenuated by applying the proposed controller.

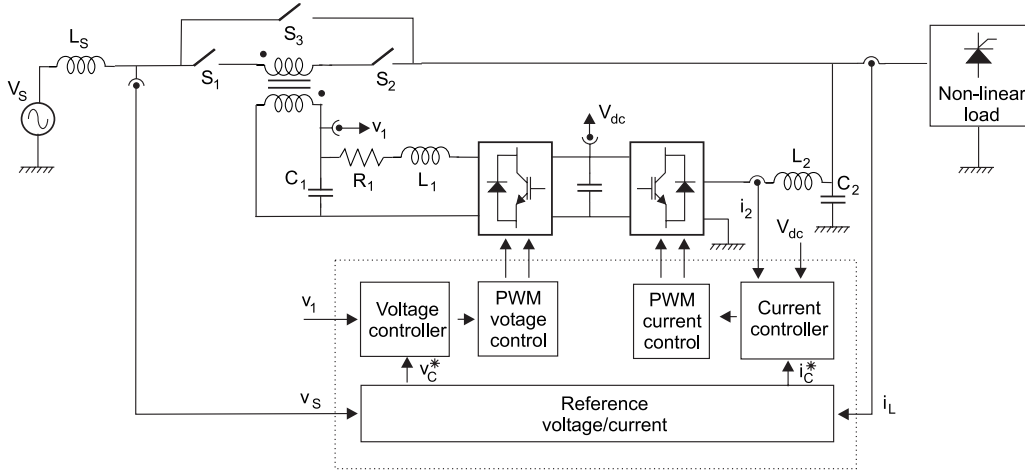


Fig. 2. General structure of UPOC controllers

2. Functional structure of UPQC

The basic functionalities of a UPQC controller are depicted in figure 2. The voltage compensation (v_c^*) and current injection (i_c^*) reference signals, required for compensation purposes, are evaluated from the instantaneous measurements of the source voltage (v_s), the dc-bus voltage (v_{dc}) and the load current (i_L). These reference signals are compared to the measured feedback signals v_1 and i_2 and applied to the decoupled voltage and current controllers, which ensure that the compensation signals correspond to the reference ones. The gate signals of the power converters are obtained by applying pulse width modulators to the controller outputs. The power converters switch at high frequency generating a PWM output voltage waveform which must be low-pass filtered (L_1 , R_1 and C_1 in case of series APF and L_2 y C_2 for the shunt APF). Switches S_1 , S_2 and S_3 control the compensation status of the UPQC.

The voltage controller can be implemented in three ways. Feedback structures allow a good stationary response while forward structures generate quick responses during voltage transients. Feed-forward structures allows both behaviors being more used [9]. The generation of the reference signal depends strongly on the compensation objectives: voltage dips, over-voltages or voltage harmonics. The rms value of the grid voltage can be measured to detect voltage dips and over-voltages, once detected, the PLL used to synchronize the compensation signal must be frozen (not applied to the voltage signal) to maintain the previous phase. When the load voltage harmonics are the compensation objective, a repetitive controller can be applied to mitigate the effect of all voltage harmonics [9]. In this case the reference signal is generated inside the voltage controller and doesn't allow selective harmonic compensation, both in harmonic order and harmonic magnitude.

Different approaches have been proposed for current control of grid-connected voltage source converters. Hysteresis controllers are implemented by means of simple analog circuits but, as drawback, the spectrum of the output current is not localized, which complicates the

output filter design [10]. PI controllers have been widely applied but, due to their finite gain at the fundamental grid frequency, they can introduce steady state errors. This can be solved by means of generalized integrators [11]. Fuzzy logic and artificial neural networks (ANN) has been also proposed as current controllers in case of multiple harmonic frequencies in the reference current signal [12][13].

3. Proposed Technique for the Estimation of the Compensation Reference Signals

A. Reference voltage estimation

The structure of the proposed algorithm for estimation of v_c^* can be seen in figure 3. A stationary frame discrete Kalman filter estimates the instantaneous values of each grid voltage harmonic $v_{i,\alpha}(k)$ [14]. These voltage harmonic components are used to establish the presence of a voltage disturbance comparing the measured values and the established configuration values. Voltage dips and over-voltages are detected using the grid voltage fundamental harmonic component, the amplitudes of other measured voltage harmonic components are evaluated to establish the presence of harmonic distortion to be compensated. Once a certain voltage disturbance is detected, the series APF of the UPQC is switched-on using S_1 , S_2 and S_3 . The reference signal $v_i^*(k)$ at each required frequency is obtained as difference of the measured voltage harmonic components and the established configuration values.

The discrete Kalman filter uses a stationary frame voltage signal model, then, each voltage harmonic component at time instant k can be described as:

$$\mathbf{x}_{k+1} = \mathbf{A}\mathbf{x}_k + \mathbf{w}_k \quad (1)$$

Being:

$$\mathbf{x}_k = \begin{pmatrix} v_{1\alpha} \\ v_{1\beta} \\ \vdots \\ v_{n\alpha} \\ v_{n\beta} \end{pmatrix}_k \quad \mathbf{A} = \begin{pmatrix} M_1 & 0 & \dots & 0 \\ 0 & \ddots & & \vdots \\ \vdots & & \ddots & 0 \\ 0 & \dots & 0 & M_n \end{pmatrix} \quad (2)$$

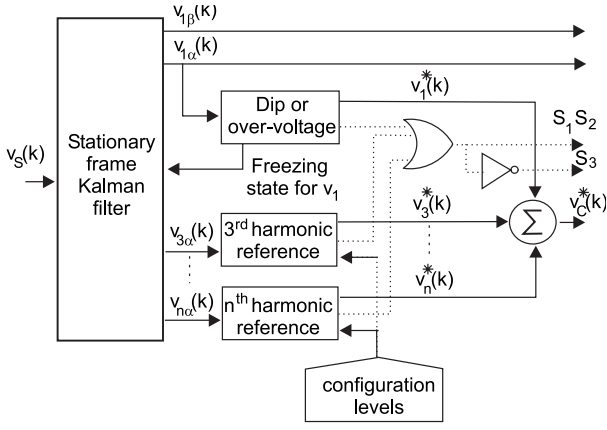


Fig. 3. Reference voltage estimator.

Where $v_{i\alpha}$ and $v_{i\beta}$ correspond respectively to the in-phase and the in-quadrature components of the fundamental frequency voltage harmonic of order i , \mathbf{w}_k is the signal model noise vector and \mathbf{M}_i is defined as:

$$\mathbf{M}_i = \begin{pmatrix} \cos(i\omega T_s) & -\sin(i\omega T_s) \\ \sin(i\omega T_s) & \cos(i\omega T_s) \end{pmatrix} \quad (3)$$

Being ω the angular frequency of the fundamental grid voltage harmonic component and T_s the sampling time of the proposed discrete algorithm.

The applied recursive discrete Kalman filtering loop corresponds to equations [5]:

$$\mathbf{P}_{k|k-1} = \mathbf{A}\mathbf{P}_{k-1|k-1}\mathbf{A}^T + \mathbf{Q}_{k-1} \quad (4)$$

$$\mathbf{G}_k = \mathbf{P}_{k|k-1}\mathbf{C}^T(\mathbf{C}\mathbf{P}_{k|k-1}\mathbf{C}^T + \mathbf{R})^{-1} \quad (5)$$

$$\mathbf{P}_{k|k} = (\mathbf{I} - \mathbf{G}_k\mathbf{C})\mathbf{P}_{k|k-1} \quad (6)$$

$$\hat{\mathbf{x}}_{k|k-1} = \mathbf{A}\hat{\mathbf{x}}_{k-1|k-1} \quad (7)$$

$$\hat{\mathbf{x}}_{k|k} = \hat{\mathbf{x}}_{k|k-1} + \mathbf{G}_k(v_{sk} - \mathbf{C}\hat{\mathbf{x}}_{k|k-1}) \quad (8)$$

where $\mathbf{P}_{k|k+1}$ is the estimation of process covariance matrix at time instant k using its value at time instant $k-1$, \mathbf{Q}_{k-1} is the variance matrix associated to vector \mathbf{w}_k , \mathbf{G}_k is the Kalman gains matrix at time instant k , vector \mathbf{C} , using this signal model, is defined as:

$$\mathbf{C} = (1 \ 0 \ \dots \ 1 \ 0) \quad (9)$$

\mathbf{R} is the variance matrix of the voltage measurement error and $\hat{\mathbf{x}}_{k|k-1}$ is the prediction of voltage harmonic components in the stationary frame $\alpha\beta$ at time instant k using the estimation at time instant $k-1$ $\hat{\mathbf{x}}_{k-1|k-1}$.

The amplitude of the fundamental voltage harmonic component at instant k is evaluated as:

$$V_1(k) = \sqrt{v_{1\alpha}^2(k) + v_{1\beta}^2(k)} \quad (10)$$

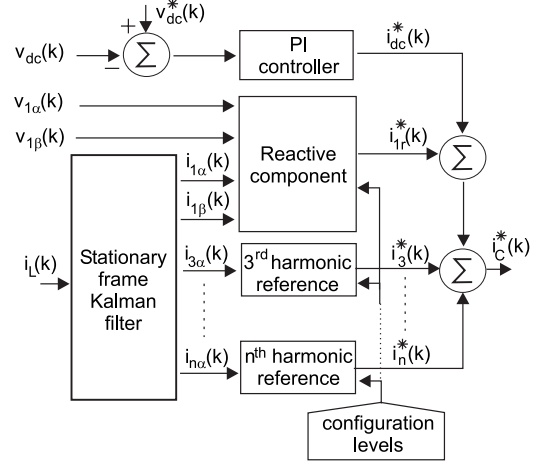


Fig. 4. Reference current estimator.

which is compared with the required load voltage. When a voltage dip or over-voltage is detected the recursive Kalman filter is frozen at the fundamental frequency and the described filtering loop is reduced to (7) at the fundamental harmonic component, using previously buffered values of $v_{1\alpha}(k)$ and $v_{1\beta}(k)$. The compensation reference signal at the fundamental frequency is obtained as:

$$v_1^*(k) = \frac{V_1^R - V_1(k)}{V_1^R} v_{1\alpha}(k) \quad (11)$$

where V_1^R is the required load voltage amplitude. The compensation references for higher order harmonic components of $v_s(k)$ are only applied when the established configuration levels are reached. These signals are obtained as:

$$v_i^*(k) = \frac{\sqrt{v_{i\alpha}^2(k) + v_{i\beta}^2(k)} - V_i^R}{\sqrt{v_{i\alpha}^2(k) + v_{i\beta}^2(k)}} v_{1\alpha}(k) \quad (12)$$

where V_i^R is the configuration amplitude of the voltage harmonic with order $i > 1$.

Finally, the complete compensation reference signal at instant k can be obtained using:

$$v_c^*(k) = \sum_{i=1}^n v_i^*(k) \quad (13)$$

Where each $v_i^*(k)$ depends on the established configuration level V_i^R , allowing the selective compensation of voltage disturbances

B. Reference current estimation

The process to obtain i_c^* is shown in figure 4. A discrete Kalman filter using a stationary frame is applied to the load current i_L in order to obtain its harmonic and reactive components. The compensation levels for these components can be established using the configuration levels block depicted in the figure. The estimation of the harmonic current references is carried out according to

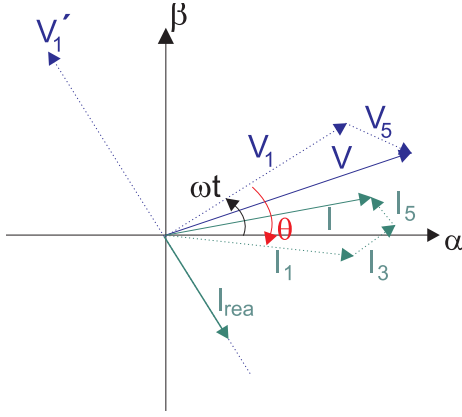


Fig. 5. Representation of voltage and current phasors in the synchronized stationary reference frames

the process described in the previous section and, hence, this section only describes the estimation of the load current component which contributes to the reactive power. It must be considered that the dc-bus voltage is controlled by means of a current consumption at the fundamental grid frequency, whose amplitude is determined through a PI controller, and in-phase with the source voltage.

Since the controller executes simultaneously both Kalman filtering loops applied to load current and voltage signals, the filter reference frames will be synchronized. Under this condition the phasors corresponding to voltage and current signals are shown in figure 5. Considering the outputs of the Kalman filtering loops at the fundamental pulsation ($v_{1\alpha}(k)$, $v_{1\beta}(k)$, $i_{1\alpha}(k)$ and $i_{1\beta}(k)$):

$$v_{1\alpha}^k = |\bar{V}_1^k| \cos \frac{2\pi}{N} k \quad (14)$$

$$v_{1\beta}^k = |\bar{V}_1^k| \sin \frac{2\pi}{N} k \quad (15)$$

$$i_{1\alpha}^k = |\bar{I}_1^k| \cos \left(\frac{2\pi}{N} k - \theta \right) \quad (16)$$

$$i_{1\beta}^k = |\bar{I}_1^k| \sin \left(\frac{2\pi}{N} k - \theta \right) \quad (17)$$

where :

$$\cos \left(\frac{2\pi}{N} k \right) = \frac{v_{1\alpha}^k}{\sqrt{(v_{1\alpha}^k)^2 + (v_{1\beta}^k)^2}} \quad \cos \left(\frac{2\pi}{N} k - \theta \right) = \frac{i_{1\alpha}^k}{\sqrt{(i_{1\alpha}^k)^2 + (i_{1\beta}^k)^2}} \quad (18)$$

$$\sin \left(\frac{2\pi}{N} k \right) = \frac{v_{1\beta}^k}{\sqrt{(v_{1\alpha}^k)^2 + (v_{1\beta}^k)^2}} \quad \sin \left(\frac{2\pi}{N} k - \theta \right) = \frac{i_{1\beta}^k}{\sqrt{(i_{1\alpha}^k)^2 + (i_{1\beta}^k)^2}} \quad (19)$$

Due to the fact that:

$$\cos \left(\frac{2\pi}{N} k - \theta \right) = \cos \left(\frac{2\pi}{N} k \right) \cos(\theta) + \sin \left(\frac{2\pi}{N} k \right) \sin(\theta) \quad (20)$$

$$\sin \left(\frac{2\pi}{N} k - \theta \right) = \sin \left(\frac{2\pi}{N} k \right) \cos(\theta) - \cos \left(\frac{2\pi}{N} k \right) \sin(\theta) \quad (21)$$

the instantaneous values of the sinus and cosinus of θ can be obtained as a function of $v_{1\alpha}(k)$, $v_{1\beta}(k)$, $i_{1\alpha}(k)$ and $i_{1\beta}(k)$:

$$\cos \theta = \frac{v_{1\alpha}^k i_{1\alpha}^k + v_{1\beta}^k i_{1\beta}^k}{\sqrt{(v_{1\alpha}^k)^2 + (v_{1\beta}^k)^2} \sqrt{(i_{1\alpha}^k)^2 + (i_{1\beta}^k)^2}} \quad (22)$$

$$\sin \theta = \frac{v_{1\beta}^k i_{1\alpha}^k - v_{1\alpha}^k i_{1\beta}^k}{\sqrt{(v_{1\alpha}^k)^2 + (v_{1\beta}^k)^2} \sqrt{(i_{1\alpha}^k)^2 + (i_{1\beta}^k)^2}} \quad (23)$$

As a consequence, the magnitude of the current component which contributes to the reactive power at the fundamental grid frequency can be evaluated each sampling interval as a function of the Kalman filtering outputs:

$$|\bar{I}_{rea}^k| = |\bar{I}_1^k| \sin \theta = \frac{v_{1\beta}^k i_{1\alpha}^k - v_{1\alpha}^k i_{1\beta}^k}{\sqrt{(v_{1\alpha}^k)^2 + (v_{1\beta}^k)^2}} \quad (24)$$

In order to obtain the reference current which matches the instantaneous values of the current component contributing to the reactive power at the fundamental grid frequency, a unitary vector in phase with V_1' must be applied to (24) :

$$i_r^k = |\bar{I}_{rea}^k| \frac{\bar{V}_1^{1,k}}{|\bar{V}_1^{1,k}|} = \frac{(v_{1\beta}^k i_{1\alpha}^k - v_{1\alpha}^k i_{1\beta}^k)}{(v_{1\alpha}^k)^2 + (v_{1\beta}^k)^2} v_{1\beta}^k \quad (25)$$

The percentage of the reactive power at the fundamental grid frequency that can be compensated can be adjusted by including a factor $I_1^r \in [0, 1]$ in (25):

$$i_r^k = I_1^r \frac{(v_{1\beta}^k i_{1\alpha}^k - v_{1\alpha}^k i_{1\beta}^k)}{(v_{1\alpha}^k)^2 + (v_{1\beta}^k)^2} v_{1\beta}^k \quad (26)$$

4. Simulation Results

The proposed algorithm has been tested in simulation, using the *SimPowerSystems BlockSet* from *MatLab*, according to figure 2. The dc voltage reference of the UPQC has been established at 400Vdc, the output filter of the voltage compensator consists of a low-pass filter with $L_1=3$ mH, $R_1=1.0$ Ω and $C_1=230$ μ F while the current link of the current compensator has been modeled by applying $L_2=10$ mH and $R_2=0.8$ Ω . The nominal power of the voltage injection transformer is 12 kVA with a primary and magnetization impedances of $L_p=0.17$ mH, $R_p=35$ m Ω , $L_m=252$ mH and $R_m=80$ Ω . The source voltage contains a 50Hz 325 V signal and a 5th harmonic of 5%. A diode rectifier with a RC load ($C_L=1000$ μ F, $R_L=300$ Ω) has been used as local load.

The reference estimation technique has been applied using $T_s=156$ μ s as sampling time, the load current signal has been modeled through the first 10 odd harmonics while 1st, 3rd, 5th, 7th and 9th voltage harmonics has been considered in case of the grid voltage signal.

Fig. 6 shows the current compensation capabilities of the proposed UPQC controller. The voltage signal at the load terminals is shown in fig. 6.a. As can be seen, the series

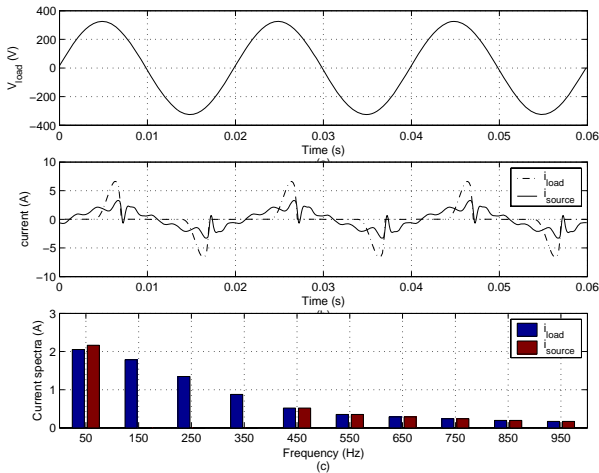


Fig. 6. Voltage waveform at the load terminals, b) load and source current waveforms with shunt compensation (only 3rd, 5th and 7th current harmonics) and c) load and current spectra

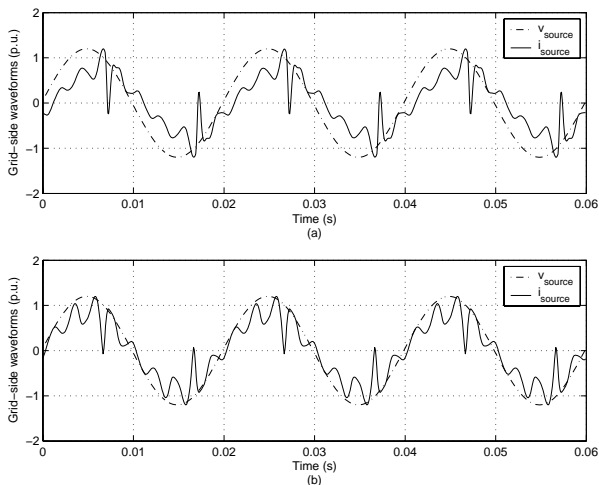


Fig. 7. Voltage and current waveform signals at the grid side a) without reactive power compensation and b) with reactive power compensation.

active filter compensates the 5th voltage harmonic resulting on a pure sinusoidal signal at the load side. The current consumption of the tested non-linear load and the source current with selective shunt compensation is shown in fig. 6.b. As can be seen the waveform quality improves due to the compensation of 3rd, 5th and 7th current harmonics. The signal spectra can be compared through fig. 6.c. As can be seen, the source current consumption at the fundamental frequency increases due to the fact that the series compensator is operating and the contribution of 3rd, 5th and 7th current harmonics to the load active power has been shifted to the fundamental grid frequency at the grid side. Moreover, the initial load current THD is reduced from 130.3% without shunt compensation to 35.9 % at the grid side. In order to improve the source current THD, more harmonic components of the load current waveform should be compensated by adjusting the selected configuration levels.

From the load voltage and current spectra, the phase displacement between the voltage waveform at the load terminals and the source current, both at the fundamental grid frequency, is 10.27° lagging (fig. 7.a.). The power factor can be improved by including in the shunt

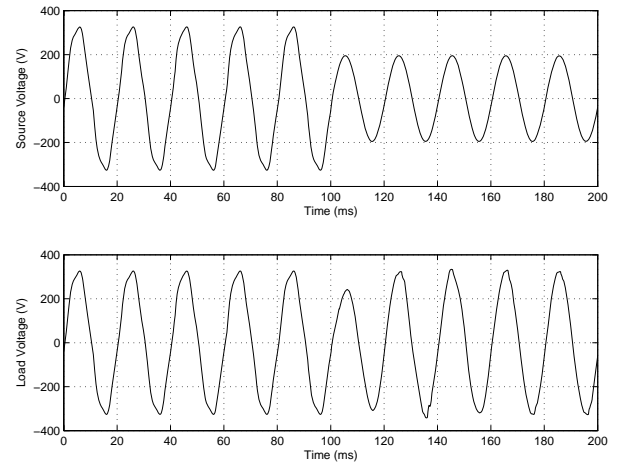


Fig. 8. Source and load voltage waveforms for a 40% voltage dip.

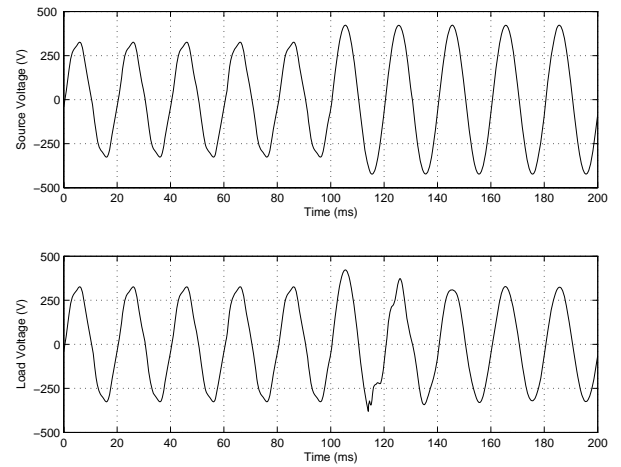


Fig. 9. Source and load voltages when a 30% over-voltage is applied

compensation targets the load current component at the fundamental grid frequency which contributes to the reactive power (fig. 7.b.). In this case, the displacement angle has been reduced to 0.1° maintaining the harmonic currents compensation capability.

The behavior of the proposed UPQC controller has been also tested under voltage dip/over-voltages. Fig. 8 shows the obtained results in case of a voltage dip is applied at $t=100$ ms with a voltage amplitude reduction up to 195 V. The response time, including the voltage dip detection time and the controller response, is less than one cycle at the fundamental frequency which confirms the appropriate behavior of the proposed UPQC control technique for the compensation of voltage dips.

Figure 9 shows the obtained simulation results when a 30% over-voltage is applied at 100 ms. As can be seen, once the over voltage is detected, the UPQC acts reducing the load voltage amplitude to the load nominal voltage and the dynamical response takes 30 ms. This demonstrates that the proposed controller allows a properly compensation of over-voltages.

Finally, the voltage harmonic compensation capability of a UPQC controlled using the proposed estimation

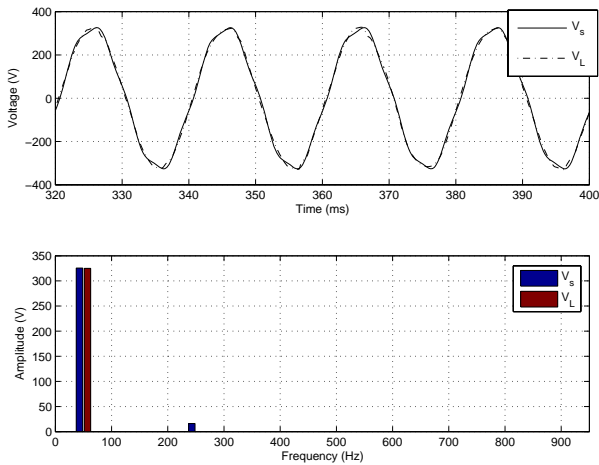


Fig. 10. Source and load voltage waveforms and spectra for the 100% compensation of the 5th voltage harmonic.

reference technique is shown in figure 10. A grid voltage (v_s) with a 5% of 5th harmonic component is applied. The tolerance level for the 5th voltage harmonic (V_s^R) is fixed to 0 V for fully compensation. The obtained results show that the proposed control technique allows the 100% mitigation of the 5th voltage harmonic component.

5. Conclusions

A new digital control technique which applies a discrete Kalman filter to generate the compensation reference signals in UPQC has been presented and tested in simulation.

The structure of the proposed reference voltage and current estimator allows the compensation of the reactive power at the fundamental grid frequency, voltage and currents harmonics simultaneously and mitigates voltage dips and over-voltages. Moreover, the disturbance compensation levels can be configured allowing a more flexible operation. The performance of the proposed controller has been evaluated through dynamical and steady-state simulation tests.

References

[1] A. Nasiri and A. Emadi, "Different topologies for single-phase unified power quality conditioners," in Proc. Of 38th IEEE Industry Applications Society Annual Meeting, vol. 2, 12-16 October 2003. pp. 976-981.

[2] L. M. Tolbert, F. Z. Peng and T. G. Habetler, "A multilevel converter-based universal power conditioner," IEEE Transactions on Industry Applications, vol. 36, no 2, March/April 2000. pp. 596- 603.

[3] G. Benysek, Improvement in the quality of delivery of electrical energy using power electronics. Springer. London. 2007.

[4] H. Akagi, E. H. Watanabe and M. Aredes, Instantaneous Power Theory and Applications to Power Conditioning. Wiley-IEEE Press. April 2007.

[5] M. Forghani and S. Afsharnia, "Online wavelet transform-based control strategy for UPQC control system," IEEE Transactions on Power Delivery, vol. 22, no. 1, January 2007. pp. 481-491.

[6] H. Fujita and H. Akagi, "The unified power quality conditioner: the integration of series- and shunt-active filters," IEEE Transactions on Power Electronics, vol. 13, no. 2, March 1998. pp. 315-322.

[7] D. Graovac, V. Katic and A. Rufer, "Power quality compensation using universal power quality conditioning system," IEEE Power Engineering Review, December 2000. pp. 58-60.

[8] B. Han, B. Bae, H. Kim and S. Baek, "Combined operation of unified power-quality conditioner with distributed generation," IEEE Transactions on Power Delivery, vol. 21, no. 1, January 2006. pp. 330-338.

[9] Y. H. Cho and S. K. Sul, "Controller design for dynamic voltage restorer with harmonics compensation function", in Proc. of 39th IAS Annual Meeting, vol. 3, October 2004. pp 1452-1457.

[10] D. G. Holmes and T. A. Lipo, Pulse width modulation for power converters : principles and practice. Wiley-IEEE Press. 2003.

[11] X. Yuan, W. Merk, H. Stemmler and J. Allmeling, "Stationary-frame generalized integrators for current control of active power filters with zero steady-state error for current harmonics of concern under unbalanced and distorted operating conditions," IEEE Transactions on Industry Applications, vol. 38, no. 2, March-April 2002. pp. 523-532.

[12] C. N. Bhende, S. Mishra and S. K. Jain, "TS-fuzzy-controlled active power filter for load compensation," IEEE Transactions on Power Delivery, vol. 21, no. 3, July 2006. pp. 1459-1465.

[13] J. H. Marks and T. C. Green, "Predictive transient-following control of shunt and series active power filters," IEEE Transactions on Power Electronics, vol. 17, no. 4, July 2002. pp. 574-584.

[14] V. Moreno and J. Barros, "Application of Kalman filtering for Continuous Real Time Tracking of Power System Harmonics", IEE Proc.- Gener. Transm. Distrib. vol. 144, no. 1, January 1997. pp 13-20.